Distance-based Characterization of Subgrid-scale Dynamic Flow Behavior for Multi-phase Flow Upscaling

Satomi Suzuki[1]

Abstract Distance-based method has been successfully applied to various kinds of geological modeling problems such as history matching, uncertainty qualification and pattern-based geostatistical simulation as an effective means of model parameterization or pattern classification. Individual reservoir models or geological patterns are parameterized as points in a space defined by a distance function which measures similarity between a pair of models or geological patterns. The reservoir models or geological patterns are positioned in this similarity space in such a way that similar ones are clustered and dissimilar ones are separated. Because of such nature of the space, statistical clustering method or search technique can be efficiently implemented. This paper proposes a new application of the distance-based method to the area of multi-phase flow upscaling.

The proposed upscaling technique relies on dynamic pseudo function method utilizing local boundary condition. The major limitation of existing methods is that different simulation gridblock obtains different pseudo function, resulting in the requirement of generation and usage of too many pseudo relative permeability curves that exceed the capability of conventional flow simulation practices. Several attempts to group pseudo functions have been made since 1990s. However, they have not yet attained enough efficiency and robustness for commercial applications. In the method proposed in this paper, we quickly generate a subgrid-scale pattern of displacement front for each simulation gridblock based on fine scale geological description. Fast static method that uses shortest-path algorithm enables such a rapid generation of displacement front profile without running flow or streamline simulation. Then, by using distance-based approach, simulation gridblocks are clustered in accordance with the similarity of the shape of displacement front. All simulation gridblocks belonging to the same cluster can share the same dynamic pseudo function because of the strong correlation between displacement front profile and pseudo relative permeability curves.

[1] ExxonMobil Upstream Research Company, PO Box 2189, URC-GW3-1028A, Houston, Texas 77252-2189, USA, e-mail: satomi.suzuki@exxonmobil.com

1 Introduction

Multi-phase flow upscaling utilizing dynamic pseudo methods has been actively investigated and applied to reservoir simulation studies for decades. Numerous variations of the methods have been proposed [1-13] and reviewed [14-17]. However, the dynamic pseudo methods are often criticized mainly because of the following reasons; first, 1) pseudo functions are strongly dependent on boundary conditions and second, 2) every different coarse gridblock and every flow direction can have different set of pseudo functions [15]. The former limitation is particularly significant if global methods and their variants [1-2, 9-12, 13] are employed for the dynamic pseudo generation. In this case, if well position and flow rate are changed, pseudo functions must be regenerated. This problem can be avoided if local methods [5-8] are utilized. However, it is usually computationally prohibitive to dynamically generate pseudo functions using local boundary condition because it requires running two-phase flow simulation on every coarse gridblock and every flow direction. Therefore, as clearly stated in [15], ‘we must assign each coarse gridblock to one of the limited number of rock types in such a way that all blocks within the same rock type have “similar” pseudos.’ However, although several authors have proposed methods for such clustering of simulation gridblocks [18-21], the methodology has not been established to the level of commercial applications.

In this paper, we propose to apply distance-based modeling [22-29] to group coarse simulation gridblocks into clusters for assigning pseudo function. The central idea of the distance-based modeling is to parameterize geological models or geological patterns in a metric space in such a way that similar ones are clustered and dissimilar ones are separated. The similarity between any two geological models/patterns is evaluated using a distance function. Based on the similarity distances measured between all pairs of geological models/patterns, the ensemble of models/patterns is accommodated in a space where models/pattern can be clustered or searched by utilizing the information of similarity. Arpat and Caers [22] introduced the concept and use of similarity distances to multi-point geostatistics (MPS) simulation utilizing geological pattern. Suzuki and Caers [23]/Suzuki et al. [24] introduced parameterization of geological models based on similarity distance to the solution of inverse problems in order to invert geological concept and structural geometry of reservoirs, respectively, from historical production data. Scheidt and Caers [25–26] developed a methodology of uncertainty quantification of reservoir performance by integrating distance-based method with kernel clustering. This method is also applied to more complex geological settings by Alpak et al. [27]. Park and Caers [28] extended the distance-based modeling to the solution of spatial inverse problems in high-dimensional space. Honarkhah and Caers [29] applied the distance-based modeling to facilitate multi-point geostatistics (MPS) simulation with pattern [22]. In most cases, direct evaluation of similarity between models in terms of characteristic of interest (e.g. flow response) is computationally prohibitive. Hence a surrogate of similarity distance is typically utilized. For example, if one desires to cluster reservoir models based on the similarity of flow response, a surrogate of flow response, such as streamline simulation result, can be utilized [25-28] instead of flow simulating all reservoir models in the ensemble. The key component of the workflow design strategy is to ensure the strong correlation between the similarity of surrogate (e.g. streamline simulation result) and the similarity of characteristics of interest (e.g. flow response from full physics flow simulation) between models/patterns.

The application of the distance-based method to multi-phase flow upscaling is motivated by the resemblance of the problem setting of the dynamic pseudo method to the workflow offered by the distance-based modeling. In order to utilize pseudo functions for multi-phase flow upscaling, one must group simulation gridblocks into clusters in such a way that all gridblocks within the same group have “similar” displacement characteristics. However, generating dynamic pseudo functions for all gridblocks is computationally prohibitive. The solution to this problem is to employ a surrogate of pseudo function in such a way that the similarity of the surrogate is strongly correlated to the similarity of pseudo. By implementing statistical clustering in a space defined by the surrogate-based similarity distance, one can group simulation gridblocks as desired. As a surrogate for the distance calculation, we utilize subgrid-scale displacement front profile which is controlled by fine scale geological description within a coarse gridblock. Such a displacement front profile can be rapidly generated without running flow simulation or streamline simulation by utilizing shortest-path algorithm [30-31]. The distance function proposed in [22] for pattern-based multi-point geostatistical (MPS) simulation is employed as a distance measure to evaluate the similarity of the pattern of displacement front. The concept of this approach has been tested using a two-dimensional cross-sectional model in our previous publication [32] and demonstrated promising results. However, it was also observed that the applicability of the method deteriorated with the increase in mobility ratio of reservoir fluids. In this paper, we enhance the methodology by improving boundary condition for generating pseudo and displacement front profile, and show that robustness of the proposed method is significantly improved. We also extend the method to three-dimensional modeling and present the application result of the multi-phase flow upscaling of Upper Ness sequence (fluvial channel system) of SPE 10 model [33].

2 Method

Fig. 1 illustrates the principal concept of the multi-phase flow upscaling method proposed in this paper. We assume that, if the pattern (or shape) of displacement front in subgrid-scale is similar between two coarse gridblocks, corresponding pseudo relative permeability curves are also similar. If this assumption is valid, a set of simulation gridblocks that exhibit similar displacement front profiles in subgrid-scale can share the same pseudo relative permeability. Fig. 2a depicts examples of the displacement front profiles generated using a rapid static method equipped with Dijkstra's shortest-path algorithm [34, 35]. Here, we utilize similar approach to the method of Hird and Dubrule [30] but employ time-of-flight (TOF) [36] and the method of Frankel [31] to predict displacement front profile for individual corase simulation gridblocks. The time-of-flight (TOF), τ, on fine scale grid (*i*, *j*, *k*) is caluculated based on the fine scale porosity and permeability as;

$$\tau(i,j,k) = \int_{inlet}^{i,j,k} \frac{\varphi}{u} ds, \tag{1}$$

where φ is porosity and u is Darcy velocity of displacing phase. By imposing the same boundary condition as utilized for dynamic pseudo generation, the shortest path that acheives the minimum time-of-flight (TOF) from the inlet is rapidly found. The corresponding TOF value is also recorded on fine scale gridblocks. Then, the image depicted in Fig. 2a, predicting the displacement front at the time of breakthrough at coarse grid interface, is obtained by thresholding the TOF value. Fig. 2b shows the water saturation distribution predicted by flow simulation on the same fine scale geological description as in Fig. 2a. As compared in the figures, although the time-of-flight (TOF) does not exactly reproduce the simulated water saturation distribution, it still captures the pattern of subgrid-scale displacement profile, which is sufficient enough for grouping pseudo functions.

Fig. 3 illustrates the distance-based modeling workflow that groups coarse scale simulation gridblocks based on the similarity of displacement front profile. First, a fine scale geological model is upgridded into a coarse scale flow simulation model. Each coarse scale gridblock is provided with displacement front profile generated using the fast static algorithm. The similarity of displacement front patterns is evaluated by a distance function, which is described later, between the pairs of gridblocks. Using the evaluated distance, a distance matrix that describes the similarity between gridblocks is constructed. The simulation gridblocks are parameterized in a metric space based on this distance matrix in such a way that similar ones are clustered and dissimilar ones are separated. The clustering of the coarse gridblocks is implemented in this distance-based space utilizing a statistical technique. In this paper, we use CLARA (Clustering LARge Applications) [37], which is one of the best known k-medoid-based clustering algorithms, for the distance-based clustering. CLARA first samples a subset of gridblocks from the entire set of gridblocks, then constructs distance matrix for this subset. The clustering is performed in this subset using PAM (Partitioning Around Medoids) algorithm [37] by finding a set of medoids (i.e., gridblocks that are located in the center of clusters in the similarity space) which achieves "best clustering" in terms of the total distance between medoids and non-medoid objects within the clusters. This process is repeated several times by changing the subset of gridblocks by random drawings. The best medoids that achieve the best result among the PAM results on the multiple sample sets are selected as final medoids. Once the final medoids are chosen, the remaining unsampled gridblocks are associated with the nearest medoids based on the similarity distance. The detailed description of CLARA and PAM algorithms is found in Ng and Han [38]. Instead of using CLARA, the distance-based method porposed by Honarkhah and Caers [29] for multi-point geostatistical (MPS) simulation can be also utilized.

Once coarse gridblocks are grouped into clusters, only one pseudo relative permeability is generated for each cluster. This upscaling is implemented by flow simulating multi-phase flow behavior on a “representative” coarse scale gridblock located in the center of the cluster (= medoid). Then the generated “representative” pseudo relative permeability curve is assigned to all gridblocks belonging to the same cluster.

To evalulate the similarity of pattern, we employ Manhattan distance [39] and Euclidean distance transform (EDT) [40] which are utilized by Arpat and Caers [22] for pattern-based MPS simulation. Fig. 4 illustrates the procedure by showing an example:

1. Convert the time-of-flight (TOF) distribution (Fig. 4a) into a binary image (Fig. 4b)
2. Using Chamfer transform [41], convert the binary image of step 1 to “distance map” through Euclidean distance transform (EDT) [40]. After the transformation, each fine gridblock of distance map receives Euclidean distance to the nearest dark pixel of Fig. 4b. (Fig. 4c)
3. Calculate Manhattan distance between a pair of the distance maps as below:

$$d_{1,2} = \sum_N \| a_i^1 - a_i^2 \|. \tag{2}$$

$d_{1,2}$: Manhattan distance between pattern 1 and pattern 2
a^1_i: value at fine gridblock *i* on the distance map from pattern 1
a^2_i: value at fine gridblock *i* on the distance map from pattern 2
N: number of fine gridblocks on pattern

Calculated Manhattan distance serves as a measure of similarity of the shape of subgrid-scale displacement front between two coarse gridblocks. The lower value of Manhattan distance corresponds to greater similarity between the patterns. Fig. 5 shows examples of similarity distance calculated for pairs of subgrid-scale displacement front profiles. The figure also depicts the comparison of corresponding pseudo relative permeability curves. As shown in the figure, the similarity distance of the pattern of displacement front profile is well correlated to the similarity of corresponding pseudo functions.

More detailed description about the method proposed in this paper is provided in our previous publication [32].

3 Improvement of Boundary Condition

The proposed method relies on dynamic pseudo generation methods using local boundary condition (= local methods) since, unlike pseudos from global methods, the pseudo relative permeability from local methods is independent on well positions, flow rate and initial saturation etc. However, as mentioned earlier, the preliminary test of the proposed method, presented in our previous publication [32], exhibited some weakness to the cases with unfavorable mobility ratio. This section discusses how the improvement of boundary condition utilized in the local method can enhance the robustness of the proposed method to the cases with unfavorable mobility ratio.

Fig. 6 compares conventional local boundary conditions (Fig. 6a), utilized in our previous publication [32], and new local boundary condition (Fig. 6b) used in this paper. In the figures, a coarse gridblock denoted as 'upstream coarse grid domain' corresponds to the simulation gridblock where dynamic pseudo function is generated. As shown in Fig. 6a, the conventional local methods impose constant saturation boundary condition of Sw = 1.0 at the inlet face of simulation gridblock where the pseudo function is generated. In fact, such a boundary condition never occurs in reservoir models unless an injector is placed at the inlet face of the gridblock. The effect of this unrealistic saturation condition tends to be exaggerated with the increase in mobility ratio. To avoid this problem and obtain more realistic profile of displacement front in subgrid-scale, we use the local boundary condition depicted in Fig. 6b. As shown, it simply attaches an upstream simulation gridblock to the gridblock where pseudo function is generated, and imposes constant saturation boundary condition of Sw = 1.0 at the inlet face of the concatenated domain. Either constant pressure or constant effective flux rate [13] can be imposed on the same position.

An enhancement of the robustness of proposed multi-phase flow upscaling method is demonstrated using a synthetic two-dimensional cross-sectional model shown in Fig. 7. The fine scale model (Fig. 7a) consists of 200 x 100 gridblocks with grid size of 10 m x 100 m in horizontal and 2 ft in vertical. This fine scale model is coarsened to a coarse scale model (Fig. 7b) comprising 20 x 10 gridblocks with grid size of 100 m x 100 m in horizontal and 20 ft in vertical. Water flooding performance is simulated placing one injector and one producer as in the figure, using constant water injection rate and constant total liquid production rate as well constraints. The dimension of the model is 2 km x 100 m x 200 ft.

Fig. 8 shows the results of the numerical experiment as a comparison of the results from the conventional boundary condition (Fig. 6a) and those from the new boundary condition (Fig. 6b). Fig. 8a compares the simulated water cut vs. time for fine scale model, coarse scale model using rock curve (= the same relative permeability as used in the fine scale model), coarse scale model using full pseudo functions, and coarse scale model using the proposed method. The results presented in Fig. 8a are obtained by using the conventional boundary condition (Fig. 6a). The full pseudo function model is built by dynamically generating pseudo relative permeability for every gridblock and every direction and assigning them as directional and irreversible relative permeability. Accordingly, total of 800 pseudo functions are utilized in the full pseudo model. The experiment is conducted by considering different mobility ratios of M = 0.5, 2.0 and 5.0. As shown, by using the conventional boundary condition (Fig. 6a), the proposed method reproduces the simulation result from the full pseudo model by using only 15 pseudo functions, instead of using 800 pseudos, in the case with favorable mobility ratio (i.e. M = 0.5). However, the number of pseudo functions required to reproduce the full pseudo simulation increases with the mobility ratio. In the case of very unfavorable mobility ratio (i.e. M = 5.0), the proposed method still requires 105 pseudos, indicating poor clustering performance of the proposed method. Fig. 8b depicts the results of the same experiment obtained using the new boundary condition (Fig. 6b). As shown in Fig. 8b, due to the more realistic representation of subgrid-scale displacement front profile, the number of pseudo functions required to reproduce the full pseudo simulation is dramatically reduced regardless of the mobility ratio of the fluids. The proposed method can reproduce the full pseudo simulation by using only 10 pseudo functions instead of 800 in the case of M = 0.5 and by using only 25 pseudos in both cases of M = 2.0 and 5.0, because of the enhanced clustering power of the methodology.

4 Application Results

We demonstrate the numerical application of the proposed method using two types of three-dimensional reservoir models. The first example utilizes a synthetic reservoir case of five-spot water injection. In this example, we also build a full pseudo model for validation purpose and compare the result simulated using the proposed method against the full pseudo simulation result. The mobility ratio of the fluids of this example is 2.0. The second application example is demonstrated using the Upper Ness sequence of SPE 10 model [33]. The mobility ratio of the SPE 10 model is 10.0. Since full pseudo generation is not practical for the SPE 10 model, the result from the proposed method is compared to fine scale simulation result in the second example.

Five-Spot Pattern Model

Fig. 9 depicts permeability distribution of fine scale model (Fig. 9a) and coarse scale model (Fig. 9b) utilized in the first numerical example. Fine scale model comprises 40x40x40 gridblocks. The size of gridblock is 30m in horizontal and 2 ft in vertical. The model is built as a pattern model for simulating five-spot water injection by placing a quarter well producer and a quarter well injector. The fine scale model is upscaled to the coarse scale model of 8x8x4 gridblocks by uniform coarsening. Transmissibility is dynamically upscaled using the pressure solver method. More aggressive coarsening compared to usual practices is applied in this example so that the construction of full pseudo model is still affordable. Water flooding performance is simulated for 30 years by imposing constant injection rate of 8400 BBL/D and constant liquid production rate of 8000 BBL/D. Four different well placements are tested as depicted in Fig. 10. Mobility ratio of the fluids is 2.0.

Fig. 11 compares simulated water cut vs. time for fine scale model, coarse scale model using rock curve, coarse scale model using full pseudo functions, and coarse scale model using the proposed method. The figure shows the results with four different well positions (Cases 1~4) depicted in Fig. 10. The full pseudo model utilizes different pseudo relative permeability for every different gridblock and different flow directions, thus requires 1,536 pseudo functions (= 8x8x4 gridblocks x 6 directions). The proposed method clusters simulation gridblocks into 15 clusters for assigning horizontal pseudo relative permeability and 5 clusters for vertical pseudo relative permeability. Accordingly, total of 20 pseudo functions are utilized in the coarse scale model using the proposed method. As illustrated in the figure, coarse scale simulation using rock curve exhibits significant delay of water breakthrough compared to fine scale simulation. By using pseudo functions, fine scale simulation result is better reproduced in all cases. Relatively poor reproduction of fine scale simulation in Case 1 is presumably because of the excessively aggressive coarsening of gridblocks. In all cases, the proposed method successfully reproduces the full pseudo simulation by using only 20 pseudo functions instead of using 1,536 pseudos.

SPE 10 Model (Upper Ness Sequence)

The proposed method is applied to multi-phase flow upscaling of Upper Ness sequence of SPE 10 model [33]. Fig. 12 illustrates horizontal permeability of fine scale model (Fig. 12a) and coarse scale model (Fig. 12b). The fine scale model consists of 56x208x50 gridblocks. In this application example, the fine scale gridblock size is horizontally enlarged from 20 ft x 10 ft x 2ft in [33] to 60 ft x 30 ft x 2 ft in order to reduce the computational burden of fine scale simulation. The model is coarsened to 14x26x10 gridblocks through uniform coarsening. The

horizontal permeability is upscaled using power averaging method [42] with ω of 0.8 and the vertical permeability is upscaled using arithmetic-harmonic method. Fluid properties and relative permeability (= rock curve) are the same as described in [33], thus the mobility ratio of the fluids is 10.0. Water injection performance is simulated for 40 years by placing one producer and one injector, imposing constant injection rate of 1010 BBL/D and constant liquid production rate of 1000 BBL/D. Six different well locations, Cases 1~6 as depicted in Fig. 13, are tested.
Fig. 14 compares simulated water cut vs. time for fine scale model, coarse scale model using rock curve and coarse scale model using the proposed method for Cases 1~6. The full pseudo model is unable to be built since it requires 21,840 pseudo functions. Hence the results from the coarse scale model using the proposed method are compared to the fine scale simulation results. The proposed method clusters coarse simulation gridblocks into 30 groups for horizontal pseudos and 5 groups for vertical pseudos, thus the total of 35 pseudo functions are utilized. As shown in Fig. 14, the proposed method reproduces fine scale simulation results by using only 35 pseudo functions in all cases, while the coarse scale simulation using rock curve exhibits the delay of water production. Fig. 15 depicts cross-sectional views of simulated water saturation distribution at 10 years after the start of production (Case 1), as a comparison among fine scale simulation (Fig. 15a), coarse scale simulation using rock curve (Fig. 15b) and coarse scale simulation using the proposed method (Fig. 15c). The cross-section shown in the figure corresponds to the plane which cuts through the positions of producer and injector. As illustrated, the proposed method better captures the pattern of sweep exhibited in the fine scale simulation than the coarse scale simulation using rock curve.

5 Conclusions

New application of distance-based modeling method to multi-phase flow upscaling is presented. The proposed method clusters coarse scale simulation gridblocks into manageable number of groups in such a way that the gridblocks belonging to the same group can share the same pseudo function. Such clustering is achieved by capturing the subgrid-scale two-phase flow characteristics of individual simulation gridblocks by predicting displacement front profile using rapid static method, and then performing statistical clustering in the space defined by distance function which measures the similarity of flow characteristics between gridblocks. It is also shown that the improvement of boundary condition for the local dynamic pseudo method significantly enhances clustering power of the proposed method. The method is applied to three-dimensional synthetic pattern model and Upper Ness sequence of SPE 10 model. Successful reproduction of full pseudo simulation and/or fine scale simulation with dramatically reduced number of pseudo functions is demonstrated.

Bibliography

[1] Jacks, H. H., Smith, O. J., and Mattax, C. C., “The Modeling of a Three-Dimensional Reservoir with a Two-Dimensional Reservoir Simulator – The Use of Dynamic Pseudo Functions,” SPE 4071, SPE Journal, June 1973, 175-185.

[2] Kyte, J. R., Berry, D. W., “New Pseudo Functions To Control Numerical Dispersion,” SPE 5105, SPE Journal, August 1975, 269-276.

[3] Hewett, T. A., Yamada, T., “Theory for the Semi-analytical Calculation of Oil Recovery and Effective Relative Permeabilities Using Streamtubes,” Advances in Water Resources, **20**(5-6), 279-292 (1997).

[4] Hewett, T. A., Archer, R. A., “Scale-Averaged Effective Flow Properties for Coarse-Grid Reservoir Simulation,” SPE 37988, SPE Reservoir Simulation Symposium, Dallas (1997).

[5] King, P. R., Muggeridge, A. H. and Price, W. G., “Renormalization Calculations of Immiscible Flow,” Transport in Porous Media **12**, 237-260 (1993).

[6] Li, Y., Efendiev, Y., Ewing, R. E., Qin, G., Wu, X. H., “An Accurate Multiphase Upscaling for Flow and Transport in Heterogeneous Porous Media,” SPE 105377, SPE Middle East Oil and Gas Show and Conference, Kingdom of Bahrain (2007).

[7] Saad, Naji, Cullick, A.S., Honarpour, M.M., “Effective Relative Permeability in Scale-Up and Simulation,” SPE 29592, Low Permeability Reservoirs Symposium, Denver (1995).

[8] Pickup, G.E., and Sorbie, K.S., “The Scaleup of Two-Phase Flow in Porous Media Using Phase Permeability Tensors,” SPE 28586, SPE Journal, **1**(4), 369-382 (1996).

[9] Suzuki, K. and Hewett, T. A., “Sequential Upscaling Method,” Transport in Porous Media **46**, 179–212 (2002).

[10] Suzuki, K. and Hewett, T. A., “Scale-Up of Relative Permeabilities of Isolated Gridblocks Accounting for Boundary Effects,” SPE 51938, SPE Reservoir Simulation Symposium, Houston (1999).

[11] Chen, Y. and Durlofsky, L. J., “Efficient Incorporation of Global Effects in Upscaled Models of Two-Phase Flow and Transport in Heterogeneous Formations,” Multiscale Model. Simul. **5**, 445-475 (2006).

[12] Chen, Y. and Li, Y., “Local-Global Two-Phase Upscaling of Flow and

Transport in Heterogeneous Formations," Multiscale Model. Simul. **8**, 125-153 (2009).

[13] Wallstrom, T.C, Hou, S., Christie, M.A., Durlofsky, L.J. and Sharp, D.H., et al., "Application of Effective Flux Boundary Conditions to Two-Phase Upscaling in Porous Media," Transport in Porous Media **46**, 155–178 (2002).

[14] Christie, M.A., "Upscaling for Reservoir Simulation," SPE37324, Journal of Petroleum Technology, **48**(11), 1004-1010 (1996).

[15] Barker, J. W., SPE, and Thibeau, S., "A Critical Review of the Use of Pseudorelative Permeabilities for Upscaling," SPE 35491, SPE Reservoir Engineering, **12**(2), 138-143 (1997).

[16] Darman, N.H., Pickup, G.E., and Sorbie, K.S., "Comparison of Two-Phase Dynamic Upscaling Methods Based on Fluid Potentials," Computational Geosciences, **6**(1), 5-27 (2002).

[17] Barker, J. W., Dupouy, P., "An Analysis of Dynamic Pseudo-relative Permeability Methods for Oil-water Flows," Petroleum Geoscience, **1**(5), 385 – 394 (1999).

[18] Dupouy, P., Barker, J. W. and Valios, J., "Grouping Pseudo Relative Permeability Curves," In Situ, **22** (1), 1-33 (1998).

[19] Christie, M. A. and Clifford, P. J., "Fast Procedure for Upscaling Compositional Simulation," SPE37986, SPE Journal, September 1998, 272-278.

[20] Chen, Y. and Durlofsky, L. J., "Ensemble-Level Upscaling for Efficient Estimation of Fine-scale Production Statistics," SPE106086, SPE Journal, December 2008, 400- 411.

[21] Chen, Y., Park, K. and Durlofsky, L. J., "Statistical Assignment of Upscaled Flow Functions for an Ensemble of Geological Models," Computational Geoscience, **15**(1), 35-51 (2011).

[22] Arpat, G. B and Caers, J., "Conditional Simulation with Patterns," Mathematical Geology, **39**(2), 177-203(2007).

[23] Suzuki, S. and Caers, J., "A Distance-based Prior Model Parameterization for Constraining Solutions of Spatial Inverse Problems," Mathematical Geosciences, **40**(4), 445-469 (2008).

[24] Suzuki, S., Caumon, G. and Caers, J., "Dynamic Data Integration for Structural Modeling: Model Screening Approach Using a Distance-Based Model Parameterization," Computational Geosciences, **12**(1), 105-119 (2008).

[25] Scheidt, C. and Caers, J., "Uncertainty Quantification in Reservoir Performance Using Distances and Kernel Methods – Application to a West Africa Deepwater Turbidite Reservoir," SPE Journal, December

2009, 680- 692.

[26] Scheidt, C. and Caers, J., “Representing Spatial Uncertainty Using Distances and Kernels,” Mathematical Geosciences, **41**(4), 397-410 (2009).

[27] Alpak, F. O., Barton, M. D. and Caers, J., “A Flow-based Pattern Recognition Algorithm for Rapid Quantification of Geologic Uncertainty,” Computational Geosciences, **14**(4), 603-621 (2010).

[28] Park, K., Caers, J., “Mathematical Reformulation of Highly Nonlinear Large-Scale Inverse Problems in Metric Space,” In: 12th European Conference on the Mathematics of Oil Recovery (ECMOR XII), September 2010, Oxford, U.K.

[29] Honarkhah, M., Caers, J., “Stochastic Simulation of Patterns Using Distance-Based Pattern Modeling,” Mathematical Geosciences, **42**(5), 487–517 (2010).

[30] Hird, K. B. and Dubrule, O., “Quantification of Reservoir Connectivity for Reservoir Description Applications,” SPE 30571, SPE Reservoir Evaluation & Engineering, February 1998, 12-17.

[31] Frankel, D., “Characterizing Connectivity in Reservoir Models Using Paths of Least Resistance,” Pat. US20070027666 A1 (2007).

[32] Suzuki, S., “Pattern-based Approach to Multiphase Flow Upscaling Using Distance-Based Clustering,” SPE 146639, SPE Annual technical Conference and Exhibition, Denver (2011).

[33] Christie, M. A. and Blunt, M. J., “Tenth SPE Comparative Solution Project: A Comparison of Upscaling Techniques,” SPE Reservoir Evaluation & Engineering, August 2001, 308-317.

[34] Dijkstra, E. W., “A Note on Two Problems in Connexion with Graphs”, Numerische Mathematik, June 1, 1959, 269-271.

[35] Siek, J. G., Lee, L., Lumsdaine, A., The Boost Graph Library: User Guide and Reference Manual, Addison-Wesley Professional, 2001.

[36] Thiele, M. R., Batycky, R. P., Blunt, M. J., Orr, R. M. Jr., “Simulating Flow in Heterogeneous Systems Using Streamtubes and Streamlines,” paper SPE 27834, SPE Reservoir Engineering, Feburary 1996, 5-12.

[37] Kaufman, L. and Rousseeuw, P. J., Finding Groups in Data: an Introduction to Cluster Analysis. John & Wiley & Sons, 1990.

[38] Ng, R.T. and Han, J., “CLARANS: A Method for Clustering Objects for Spatial Data Mining,” IEEE Transactions on Knowledge and Data Engineering, **14**(5), 1003-1016 (2002).

[39] Duda, O., Hart, P., and Stork, D., Pattern Clasification, John Wiley & Sons, Inc., New York, 2nd edition, 2001.

[40] Russ, J. C., The Image Processing Houdbook, CRC Press, 2nd edition,

1995.

[41] G. Borgefors, Distance transformations in digital images. Computer Vision, Graphics and Image Processing, **34**(3):344–371, June 1986.

[42] Srinivasan. S. and Journel, A., "Simulation of Permeability Field Conditioned to Well Test Data," SPE 49289, SPE Annual Technical Conference and Exhition, New Orleans (1998).

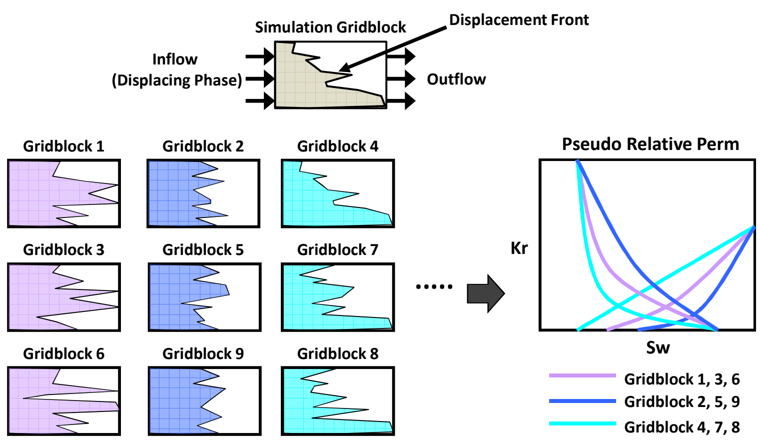

Fig. 1 Conceptual illustration of proposed multi-phase flow upscaling

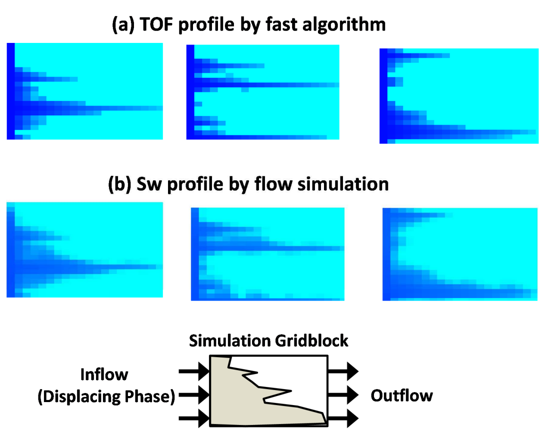

Fig. 2 Comparison between (a) displacement front profile predicted by fast static algorithm and (b) water saturation distribution from flow simulation

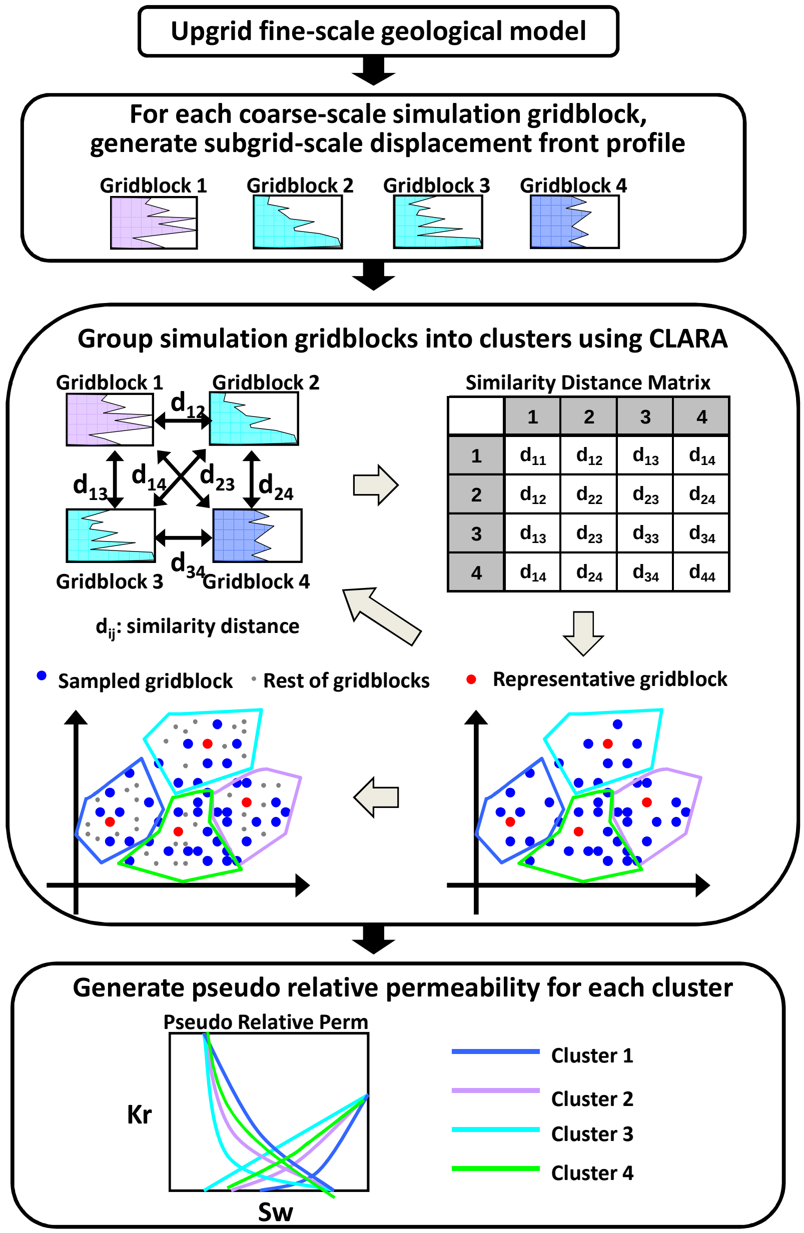

	1	2	3	4
1	d_{11}	d_{12}	d_{13}	d_{14}
2	d_{12}	d_{22}	d_{23}	d_{24}
3	d_{13}	d_{23}	d_{33}	d_{34}
4	d_{14}	d_{24}	d_{34}	d_{44}

Fig. 3 Workflow of proposed multi-phase flow upscaling using distance-based method

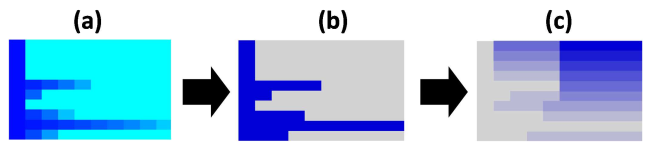

Fig.4 Euclidian distance transform (EDT) of time-of-flight (TOF) profile, (a) time-of-flight (TOF), (b) TOF converted into binary image, (c) distance map. Vertical scale is exaggerated.

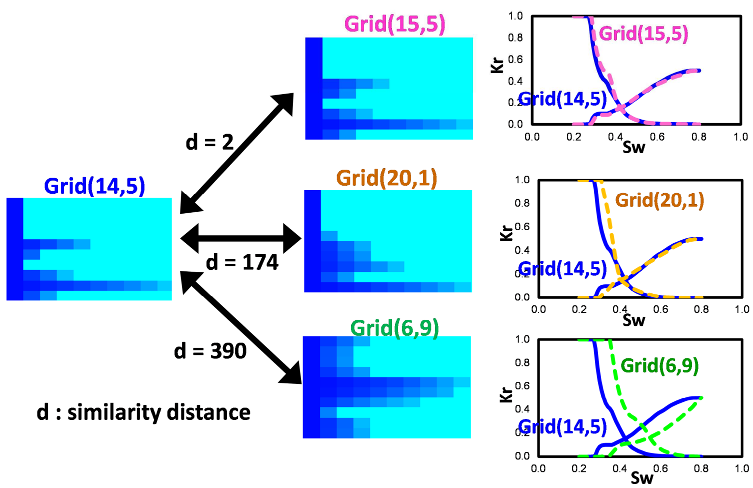

Fig. 5 Correlation between similarity distance of displacement front profile and similarity of corresponding pseudo relative permeability

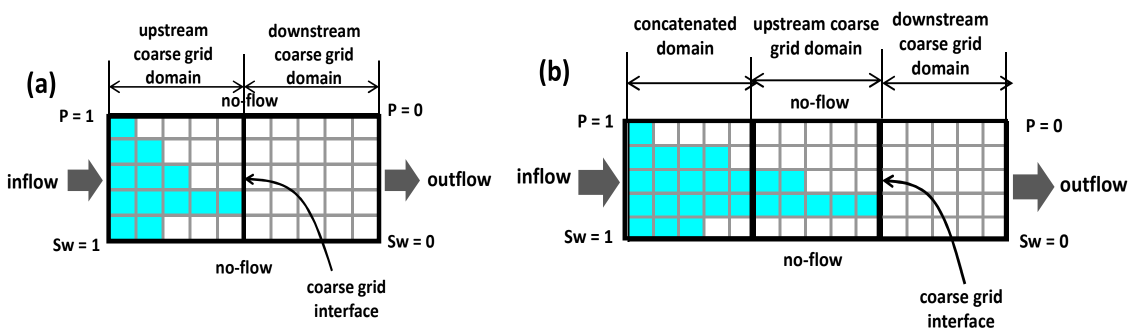

Fig. 6 Conventional boundary condition (a) and new boundary condition (b) of local methods for dynamic pseudo generation.

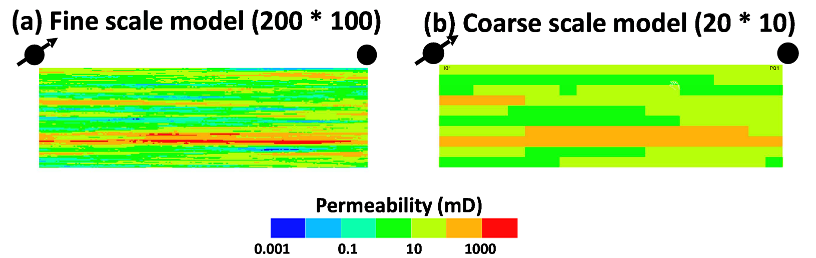

Fig. 7 Permeability distribution of fine scale model (a) and coarse scale model (b), Two-dimensional cross-sectional model

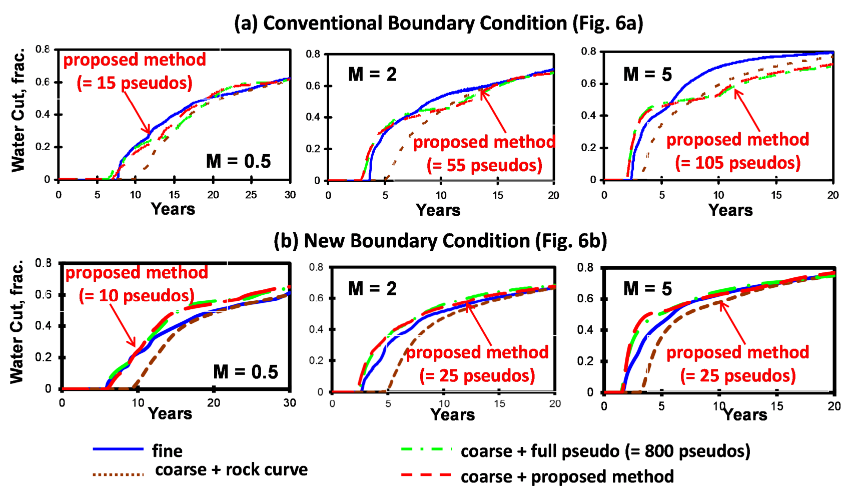

Fig. 8 Enhancement of proposed multi-phase flow upscaling method due to the improvement of boundary condition

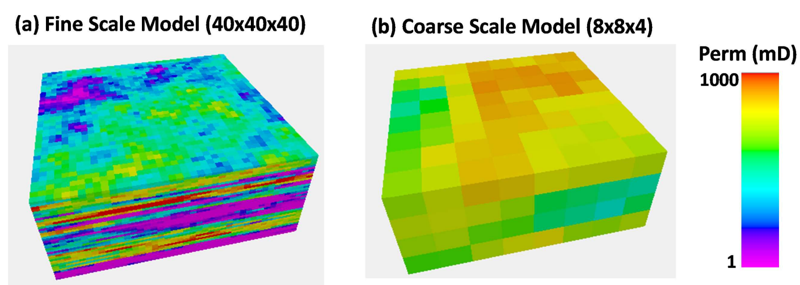

Fig. 9 Permeability distribution of fine scale model (a) and coarse scale model (b), three-dimensional 5-spot pattern model

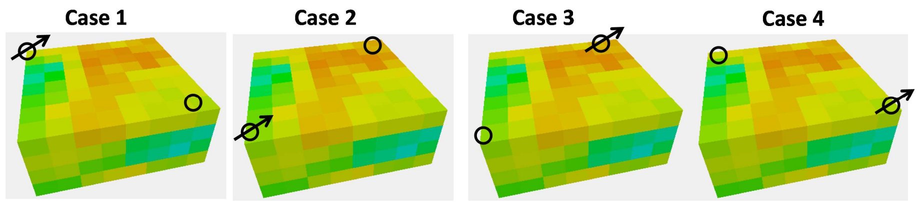

Fig. 10 Well placement, three-dimensional 5-spot pattern model, Cases 1~4

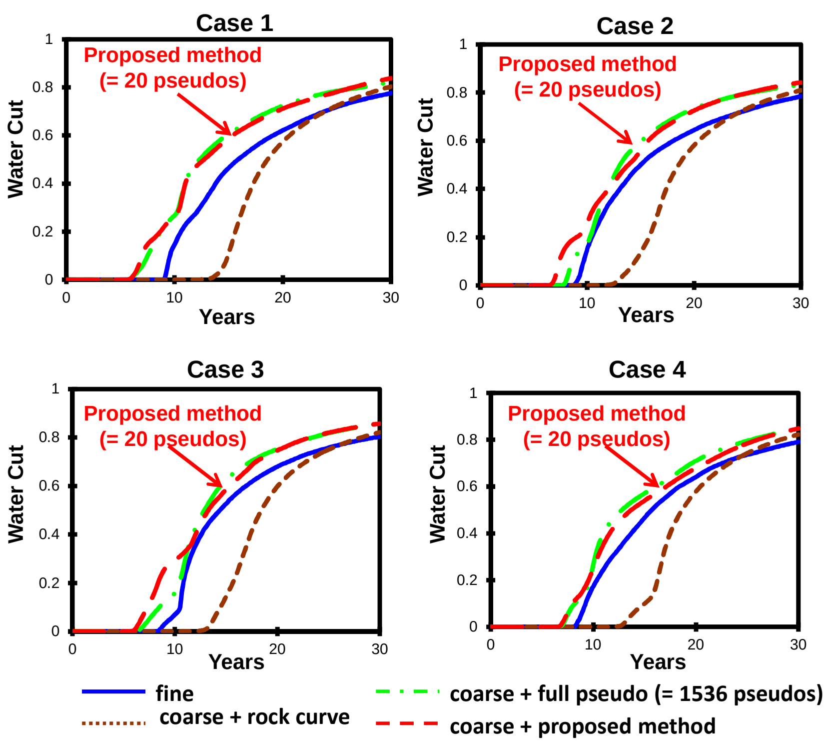

Fig. 11 Comparison of simulated water cut, three-dimensional 5-spot pattern model, Cases 1~4

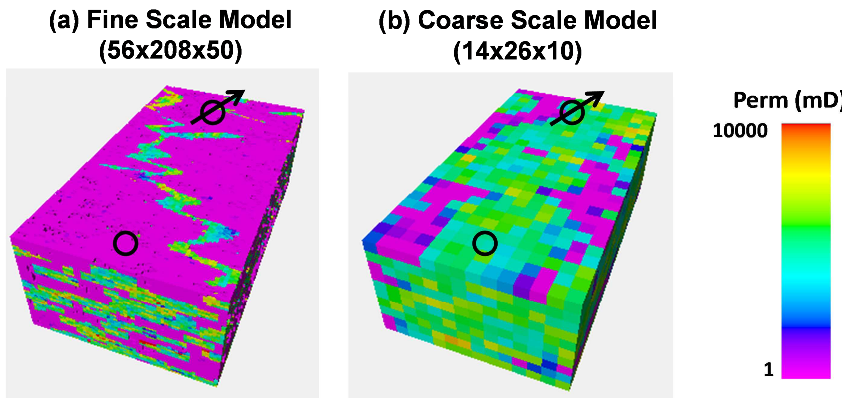

Fig. 12 Permeability distribution of fine scale model (a) and coarse scale model (b), Upper Ness sequence, SPE 10 model

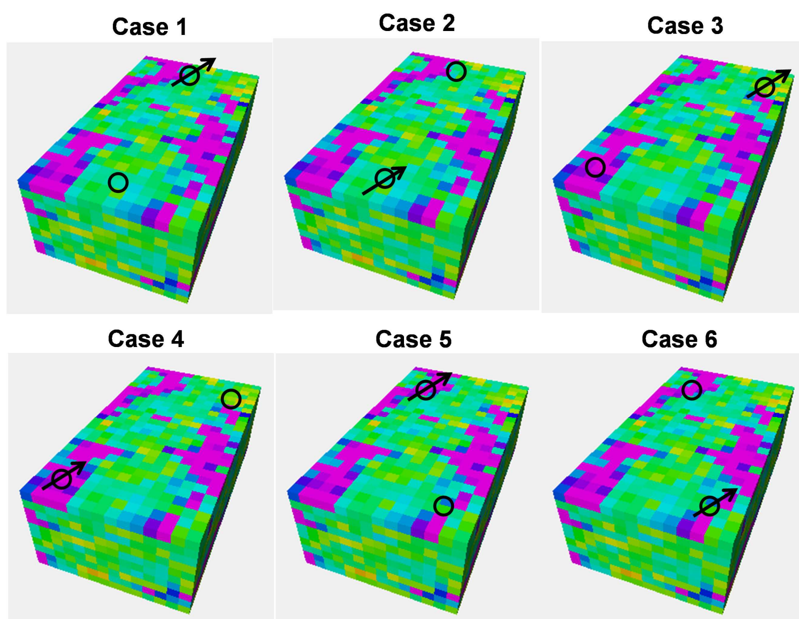

Fig. 13 Well placement, Upper Ness sequence, SPE 10 model, Cases 1~6

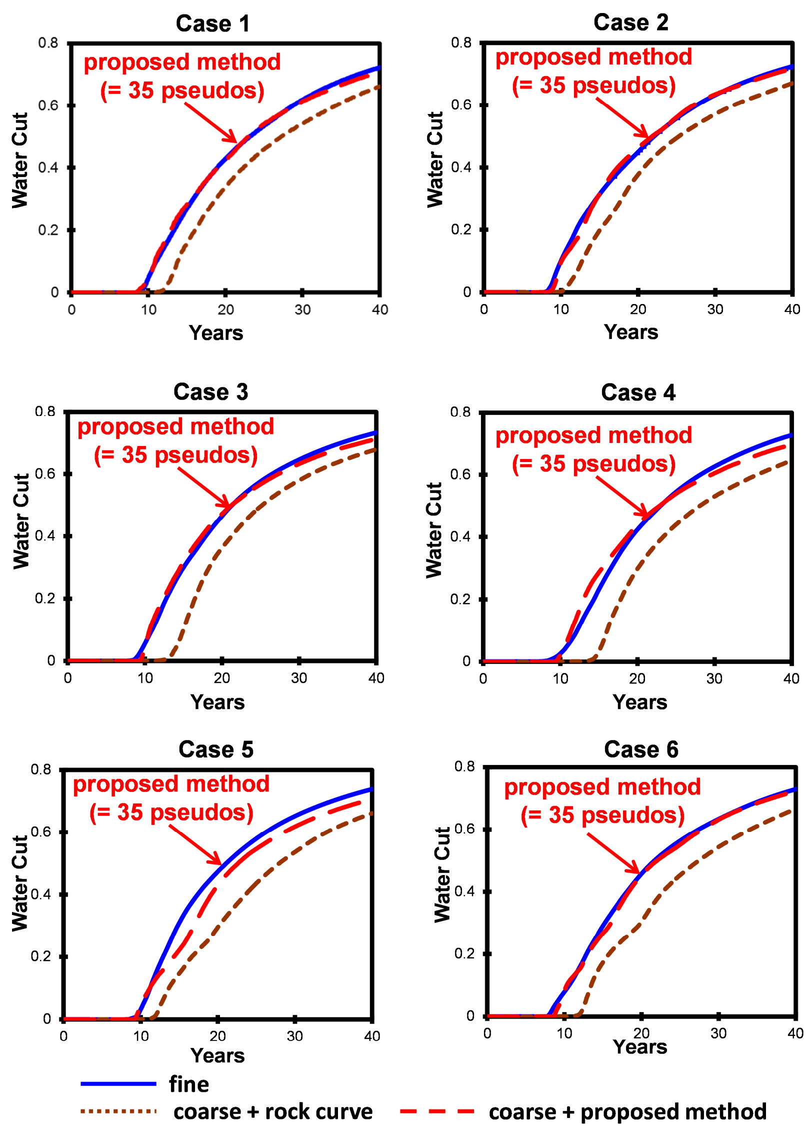

Fig. 14 Comparison of simulated water cut, Upper Ness sequence, SPE 10 model, Cases 1~6

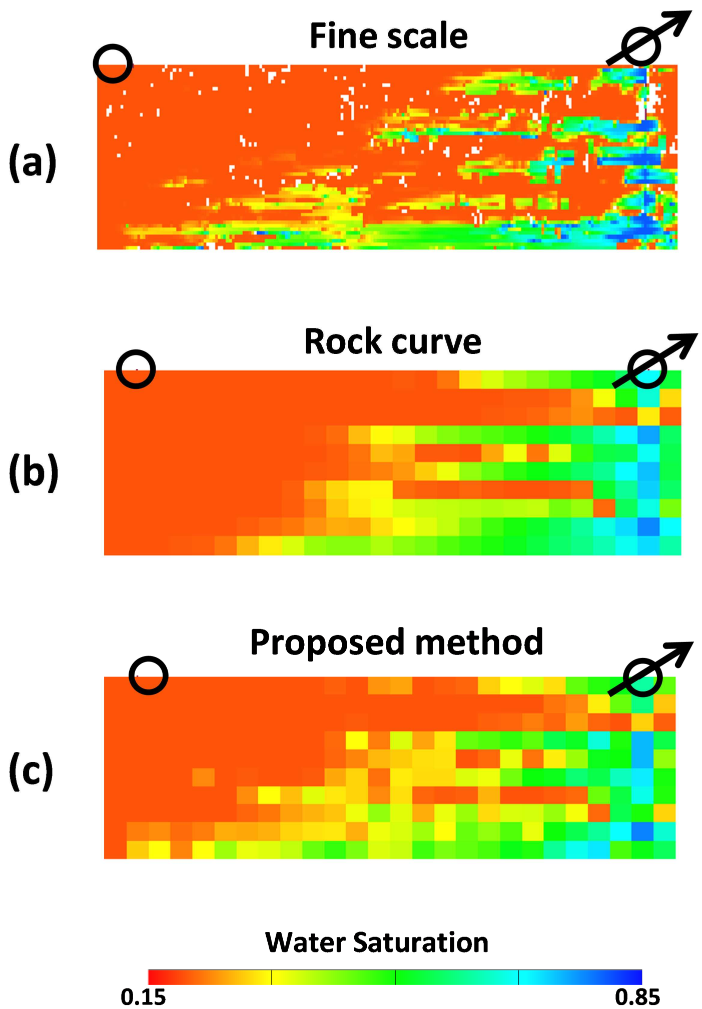

Fig. 15 Comparison of simulated water saturation distribution at 10 years after the start of production among fine scale simulation (a), coarse scale simulation using rock curve (b) and coarse scale simulation using proposed method (c), cross-sectional view, Upper Ness sequence, SPE 10 model, Case 1